ITutor/s

Dr. Arnald Grabulosa Rodríguez
Departament de Química Inorgànica i Orgànica, Secció de Química Inorgànica

Dra. Júlia Mayans Ayats
Departament de Química Inorgànica i Orgànica, Secció de Química Inorgànica

Grau de Química

Treball Final de Grau

Phosphine oxides as luminescent components for modulated emission.

Óxidos de fosfina como compuestos luminiscentes para la emisión de luz modulada.

Jeanette Carrasco Prieto

January 2023

Universitat de Barcelona

B:KC Barcelona Knowledge Campus
Campus d'Excel·lència Internacional

Si he sido capaz de ver más lejos, es porque me he parado sobre los hombros de gigantes.

Isaac Newton

Gracias al Dr. Arnald Grabulosa y la Dra. Júlia Mayans por guiarme y ayudarme en estos meses de trabajo. Gracias a todo el equipo de magnetismo molecular por brindarme su ayuda siempre que la he necesitado, en especial, a los estudiantes de doctorado Ànnia Tubau y Joan Serra.

Gracias a mis amigos y a mi familia por todo el apoyo que me han dado durante estos años de aprendizaje. En especial, a mis abuelas que siempre supieron ver lo mejor de mí, incluso ni cuando yo misma lo veía.

REPORT

IDENTIFICATION AND REFLECTION ON THE SUSTAINABLE DEVELOPMENT GOALS (SDG)

The term "green chemistry" was first used in the early 1990s. At time, it gained momentum after it received recognition and support by the US EPA (Linthorst 2010) which included innovations, creating visibility, and building networks to bring innovative products to commerce.

An important aspect of green chemistry is the design of more benign chemicals and processes that mimic nature, and take place under conditions found in nature, i.e., not requiring heat and high pressure to perform reactions. Research in line with the green chemistry principles has enabled a wide range of developments in the fields of less-toxic design of chemicals and formulations, bio-based chemicals, renewable feedstocks, safer/fewer toxic solvents and reagents, atom economy, green polymers, and other areas.

The Sustainable Development Goals (SDGs) are a set of global goals for a fair and sustainable health at all levels: form the planetary biosphere to the local community. The aim is to end poverty, protect the planet and ensure that all people enjoy peace and prosperity, now and in the future. As a result, of this reflection, it was developing humanity's 2030 Agenda and the seventeen Sustainable Development Goals that incorporate under the umbrella of sustainability social, economic, and environmental that shape the development of humanity. In addition, the ODS can be grouped into 5 major areas, known as the 5Ps, which interact together to ensure sustainable development: Planet, People, Prosperity, Peace, and Partnerships.

One of the aims of this project is the research on multiproperty materials. In this TFG project have been synthetized complexes of lanthanides that can be identified with the *people* and *prosperity* within the 5Ps. Although considered to be non-essential elements for life, the lanthanides are certainly useful in biological analysis and both in diagnosis and therapy in medicine. These applications exploit not only the spectroscopic and magnetic properties of various naturally occurring lanthanides but also the activity of synthetic radioisotopes. For example, one important application of Tb(III) and Eu(III) is in the bioanalytical area is using the luminesce of the lanthanides in time-resolved fluorescence immunoassays.

Gd(III) compounds can be used in medical applications, as the Magnetic Resonance Imaging (MRI) which represents an important area in diagnostics. MRI is based on the NMR signal generated by hydrogen nuclei present in water and its changes that are dependent on the environment. The use of a contrast agent (CA) in MRI is aimed at improving the diagnostic accuracy of clinical studies by providing images that contain physiological information along with exquisitely high anatomical detail. Research is now focused on the development of new classes of Cas with improved properties such as smart CAs, target-selective CAs, and macromolecular CAs.

A disadvantage of these complexes is toxicity that they can have although lanthanide compounds are not particularly toxic. The problems of toxicity are associated with the mining and treatment (including wastes disposal) of rare earth ores, but these are largely because the ores are typically contaminated with significant levels of radioactive elements, as thorium and uranium being the most important of these. The lanthanides promethium occurs only as radioisotopes of short half-life, the longest lived being ^{145}Pm, ($t_{1/2}$ = 17.7 y) and thus its abundances is so low that it is not considered a health risk.

Finally, the ODS of seventeen that can accomplish these complexes are the good health and well-being and industries, innovation, and infrastructure.

CONTENTS

1. SUMMARY

This TFG presents the synthesis, the structural characterization, magnetic properties and/or luminescence of 4 compounds: *rac*-$BINAPO_2$ (**1**), [$Tb(acac)_3$((*R*)-$BINAPO_2$)] (**2a**), [$Gd(acac)_3$((*R*)-$BINAPO_2$)] (**3a**) and [$Eu(acac)_3$((*R*)-$BINAPO_2$)] (**4a**).These lanthanide complexes were synthesized by reaction of Tb(III), Gd(III) and Eu(III) salts with racemic and enantiopure $BINAPO_2$ (**1**), which is a chiral ligand.

The structural characterization reveals that the terbium compound (**2a**) is mononuclear with the formula [$Tb(acac)_3$((*R*)-**1**)], with **1** acting as a bidentate ligand by the phosphoryl groups. The complex is octacoordinated to 8 oxygen atoms and the coordination geometry can be described either as a square antiprism (SAPR-8) or a bicapped trigonal prism (BTPR-8).

The magnetic static measurements reveal that **2a** exhibit a high intrinsic single ion anisotropy and it does not present SIMs behaviour. Compound **3a** follows a Curie law and has an intrinsic single ion isotropic behaviour and show SIMs (Single Ion Magnet) behaviour. The SIMs behaviour can be deduced by the response AC which can be observed on the magnetic dynamic measurements. And the relaxation mechanism process of magnetization has been obtained which follows a Raman and Direct process.

The luminescent measurements were performed for compound **2a** and **4a** indicated that both complexes have an efficient sensitization effect. This fact it is due to the (*R*)-**1** ligand because is a chromophore.

Finally, the chiroptical properties have been studied for Gd(III) complexes **3a** and **3b**, containing the *R* and *S* enantiomers of **1** respectively. As expected, the two spectra are mirror images, which confirms the analogous structure of **3a** and **3b**.

Keywords: coordination chemistry, molecular magnetism, phosphine oxides, lanthanide cations, luminescence, chirality.

2. RESUMEN

En este proyecto TFG se presenta la síntesis, caracterización estructural, propiedades magnéticas y/o luminiscencia de 4 compuestos: *rac*-$BINAPO_2$ (**1**), [$Tb(acac)_3$((*R*)-$BINAPO_2$)] (**2a**), [$Gd(acac)_3$((*R*)-$BINAPO_2$)] (**3a**) and [$Eu(acac)_3$((*R*)-$BINAPO_2$)] (**4a**). Estos complejos de lantánidos fueron sintetizados con mediante la reacción de sales de Tb(III), Gd(III) and Eu(III) y el ligando $BINAPO_2$ (**1**), racémico y también ópticamente puro.

La caracterización estructural revela que el compuesto de terbio (**2a**) es mononuclear con la fórmula [$Tb(acac)_3$((*R*)-**1**)], con **1** actuando como un ligando bidentado por los grupos fosforilos. El complejo es octacoordinado a 8 átomos de oxígeno y la geometría de coordinación se puede describir como un antiprisma cuadrado (SAPR-8) o un prisma trigonal bicapado (BTPR-8).

Las mediciones estáticas magnéticas revelan que el (**2a**) exhibe una anisotropía de iones únicos de alta intrínseca y no presenta comportamiento SIM (imán de un solo ion), mientras el compuesto de Gd(III) **3a** sigue la ley de Curie y tiene un comportamiento isotrópico intrínseco de un solo ion y muestra un comportamiento de SIM. El comportamiento de los SIM puede deducirse por la respuesta AC que puede observarse en las mediciones dinámicas magnéticas. Y se ha obtenido el proceso de mecanismo de relajación de magnetización que sigue un proceso Raman y Directo.

Las mediciones luminiscentes realizadas para los compuestos **2a** y **4a** indicaron que ambos complejos tienen un efecto de sensibilización eficiente. Este hecho se debe al ligando (*R*)-**1** porque es cromóforo.

Finalmente, se han estudiado las propiedades quirópticas para los complejos **3a** y **3b** de Gd(III) que contienen los enantiómeros *R* y *S* de **1** respectivamente. Como era de esperar, los dos espectros son imágenes especulares, lo que confirma la estructura análoga de **3a** y **3b**.

Paraules clau: Química de coordinación, magnetismo molecular, óxidos de fosfina, cationes lantánidos, luminiscencia, quiralidad.

3. INTRODUCTION

Molecular materials are those formed by discrete molecules and their properties arise from the molecules themselves or from molecular cooperation.

Since molecules can present magnetic, electric, and optical proprieties –usually associated only with metals, alloys, or metal oxides–, functional molecular materials could be seen as an option to replace the conventional materials used in the technological applications [1].

Organic chemistry, coordination chemistry and supramolecular chemistry are the tools to obtain functional molecular materials. Among these, coordination chemistry implies the presence of at least one metal usually coordinated to organic ligands. This opens a wide range of possibilities in molecular materials, because the physical properties can derive of the metal, the ligands, or the interaction between them.

Today, there is a lot of research activity in the field of molecular materials. And there are examples of molecular materials that behave as conductors, semiconductors, superconductors, ferrimagnets, ferromagnets or emissive materials in the visible or infrared (IR) ranges [2].

Recently, the research field of the molecular materials has focused on the synthesis of multifunctional compounds, that is, molecules that have two or more physical properties which interact with each other. For example, compounds with magnetic and conductive properties, magnetic and chiral properties, or magnetic and luminescence properties. When these properties only co-exist without interaction, we call them multiproperty systems.

The project of this TFG was centred in multiproperty compounds which have been synthetised by coordination chemistry, specifically with lanthanide(III) cations and racemic/chiral phosphine oxides.

In the next sections, the essential concepts associated with lanthanides, magnetism, luminescence, and chirality present the complexes of this TFG are briefly explained.

3.1. LANTHANIDES

The lanthanide or lanthanoid series is composed of 15 elements with atomic numbers ranging from 57 to 71, in the 6th period (4*f*) of the *f*-block. They have very similar chemical properties with scandium and yttrium and the whole series is often referred as *rare earth* elements, since lanthanides were historically isolated from uncommon oxide-type minerals. This term, however,

is currently not recommended since they are not scarcer in Earth's crust compared to many *p*- and *d*-block elements.

The properties of lanthanide metals and their compounds are influenced by the size of the lanthanide ion, the organic ligands used and the inner nature of the *f* electrons. The normal oxidation state for all the lanthanide metals is +III and decrease in ionic radius along the series are generally responsible for the changes in their properties. Thus, knowledge and understanding of these properties and how they vary across the lanthanide series is fundamental to an understanding of the chemistry of the 4*f* elements.

In addition, for reason of size, the coordination numbers are typically larger than six, and depends on factors such as solvent, solubility, and the nature of the counterions.

The lanthanides are *f*-block elements, and the lanthanide ions have all their valence electrons that fill 4*f* orbitals. Electrons in the 4*f* subshell have their principal quantum number n = 4, their azimuthal quantum number l = 3, can have their magnetic quantum number m_l = –3, –2, –1, 0, +1, +2, +3 depending on the orbital into which they are located.

In the case of the lanthanide ions, the spectroscopic term is associated with the energy shift of the hydrogenoid energy level of the subshell due to the electronic repulsion. The degeneracy of a spectroscopic term is given by the product of the spin and orbital multiplicities (Eq.1).

$$(2 \cdot S + 1) \cdot (2 \cdot L + 1) \text{ (Eq.1.)}$$

The introduction of the spin-orbit coupling then further splits each spectroscopic term into spectroscopic levels. A spectroscopic level $^{(2S+1)}\Gamma_J$ introduces the spin-orbit quantum number *J*. The *J* quantum number presents a combination of the spin and orbital angular momentum.

Among this, lanthanides differ from the main group elements and the transition metals because of the nature of the 4*f* orbitals, which are shielded by the presence of the $5s^2$ and $5p^6$ electrons. As a result of 4*f* electrons are closer to the nucleus than the electrons in the 5*s* and 5*p* orbitals, so that they are little affected by the chemical environment.

When these ions are coordinated to ligands and form a coordination complex, the orbitals are affected by the ligand-field, but the electronic configuration is only slightly affected compared to that of the free ion, i.e., the field created by the ligands is much smaller compared to the complexes of the *d*-block elements. For this reason, the orbital moment cannot be considered negligible. Therefore, the electronic structure is determined by the interelectronic repulsions and the spin-orbit couplings.

The splitting of the electronic states is therefore almost independent of the chemical environment of the Ln(III) ion. Since the importance of the spin angular momentum and the orbital momentum are similar in the description of the terms it is necessary to define the quantum number *J*. (Eq.2. and Eq.3.)

$$J = S - L \text{ (Eq.2)}$$

$$J = S + L \text{ (Eq.3)}$$

Equation 2 correspond to the ions with a *f* electron number lower than seven, while the equation 3 corresponding to the ions with a *f* electron number higher than seven. It is noteworthy that, in the case of the Gd(III) ion its electronic configuration is $4f^7$, the orbital moment is zero (L = 0) and hence this ion does not experiment spin-orbit coupling.

Although considered to be non-essential elements for life, the lanthanides are certainly useful in biological analysis and both in diagnosis and therapy in medicine. These applications exploit not only the spectroscopic and magnetic properties of various naturally occurring lanthanides but also the activity of synthetic radioisotopes. For example, one important application in the bioanalytical area is using the luminesce of the lanthanides (typically Eu(III)) in time-resolved fluorescence immunoassays [3].

3.2. BINAP AND $BINAPO_2$

The chiral diphosphine 2,2'-bis(diphenylphosphino)-1,1'-binaphthalene (BINAP, Fig.1) was synthesised by Noyori in 1980, who was awarded with the Nobel Prize in Chemistry in 2001 [4]. Nowadays, this ligand its derivatives are some of the most important in asymmetric catalysis, especially for reductions with ruthenium(II) but also with many other reactions giving rise to the formation of a C-C bonds. Noyori claims that he prepared this ligand for its “molecular beauty”. It must be pointed out that although BINAP does not contain any stereogenic atom, the ligand is chiral because of the restricted rotation of the diphenylphosphinonaphthyl groups, a phenomenon known as atropoisomerism [5].

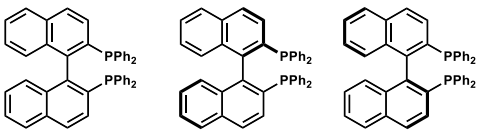

rac-BINAP *(R)-BINAP* *(S)-BINAP*

Fig.1. The structures of racemic and enantiopure isomers of BINAP.

One of the reasons that BINAP was chosen a ligand for this project is because the racemic and both enantiomers are commercially available at a reasonable price.

Phosphines such as BINAP are excellent ligands for transitions metals, in particular for soft cations such as late transition metals (Ru(II), Pd(II), Rh(I), etc.), which are very good precursors for homogeneous catalysis. In contrast, the much harder lanthanide(III) cations require ligands based on harder donors, such as N or O. For this reason, phosphine oxides are good ligands, which coordinate to the Ln(III) cations through the oxygen atom of the phosphoryl (P=O) group [6]. Therefore, in this TFG, the oxides of BINAP, known of $BINAPO_2$ (Fig.2) have been employed. Interestingly, these ligands can show good luminescent properties due to their conjugated naphthalene groups, which can act as chromophores.

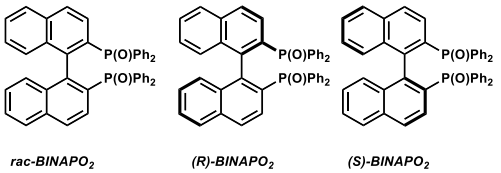

Fig.2. The structures of racemic and enantiopure isomers of $BINAPO_2$ (**1**).

The enantiopure ligands (*R* and *S*) oxides were purchased while racemic oxide is not commercially available and was prepared by oxidation of *rac*-BINAP.

3.3. MAGNETISM

Magnetic studies on coordination compounds were mostly about magneto-structural correlations and bout how paramagnetic cation (or an organic radical) behaves when a magnetic field is applied. Usually, the energy of the magnetic field applied has the order of cm^{-1} and therefore it will only affect the states derived from the ground electronic term, whose population will depend on the temperature and the Boltzmann distribution [7].

If a paramagnetic compound, with unpaired electrons, is subjected to an external magnetic field (H), it is observed that the total magnetic field measured, known as magnetic induction (B), has a larger value from the applied field (Eq.4).

$$B = H + \Delta H \quad \text{(Eq.4)}$$

This variation of H is due to the magnetization (M) of the sample. This magnetization corresponds to the density of the magnetic moments (μ) that are oriented in function of H, aligning

with the field. This orientation can only be observed preferably at low temperatures since if the temperatures are higher the thermal energy tends to disturb the preferential orientations of the magnetic moments (μ). As is shown in Fig.3 the hysteresis cycle.

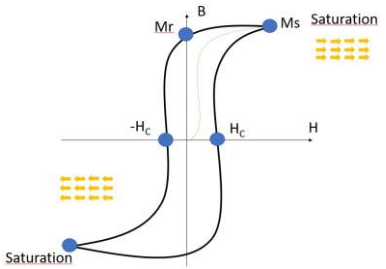

Fig.3.The hysteresis cycle. M_r is the excess magnetization, H_c is the coercive field and Ms is the saturated magnetization.

In the case of a diamagnetic compound with all the electrons paired, the external magnetic field is repelled and hence B < H, in contrast, a paramagnetic compound with unpaired electrons is attracted by the extern magnetic field (B > H).

The magnetic susceptibility (χ) is the ratio between of the magnetisation of the sample and the applied magnetic field. This parameter if the magnetic field with not too high and the temperature is low temperatures can be calculated by Eq.5:

$$\chi = \frac{M}{H} \quad \text{(Eq.5)}$$

3.3.1. Curie's Law

The Curie Law of the magnetic susceptibility applied to an isolated electron under a magnetic field (H) with a relative high temperature is given by Eq.6:

$$\chi_M T = \frac{N g^2 \beta^2}{4 K_B} \cdot \frac{W_M}{\rho} \quad \text{(Eq.6)}$$

N is corresponding to de Avogrado's number, k_B is the Boltzamann constant which is 0.695 $cm^{-1} \cdot K^{-1}$, ρ is the density ($g \cdot cm^{-3}$), W_M molecular weight ($g \cdot mol^{-1}$), g is the Landé factor and β the Bohr magneton.

The lanthanide ions are influenced by the spin magnetic moment (*S*) as the orbital moment is not zero. Then, the coupling is defined by the quantum number *J*. For Ln(III) free ions the Curie Law's is given by Eq.7:

$$\chi_M T = \frac{N g^2 \beta^2}{4 K_B} \cdot \frac{W_M}{\rho} J(J+1) \quad \text{(Eq.7)}$$

As it has been stated, the ligand field effect of the Ln(III) ions weakly modifies the static magnetic properties of compounds so it can only be observed under low temperatures, when the thermal energy decreases and the excited states are not populated [9].

3.3.2. Van Vleck Equation

John Hasbrouck Van Vleck solved the molar susceptibility equation according to the temperature, under condition of low magnetic fields and low temperatures (Eq.5). He used the perturbational method, in which the energy of the system is split according to increasingly smaller perturbations (Eq.8).

$$E_n = {E_n}^0 + H{E_n}^{(1)} + H{E_n}^{(2)} + \ldots \quad \text{(Eq.8)}$$

E_n is the total energy of the perturbed system; ${E_n}^0$ is the initial energy of the unperturbed system and $H{E_n}^{(1)}$, $H{E_n}^{(2)}$, etc. are the first second and successive Zeeman's perturbations.

The application of this equation 8 in Ln(III) ions is not possible, except for Gadolinium, since this only can be applied to isotropic compounds.

3.3.3. Single-Molecule Magnets

Single-Molecular Magnets (SMMs) are compounds with a molecular magnet behaviour, that have a fundamental magnetic state with two possible orientations, namely α and β (up-spin and down-spin). These two symmetrical states are separated by an effective energy barrier, U_{eff}. (Fig.4, left).

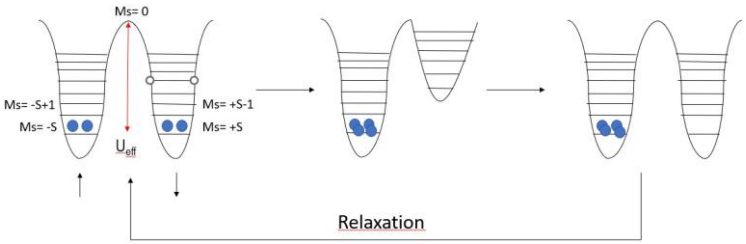

Fig.4 Double well diagram representing the potential energy when magnetic field is applied.

The U_{eff} value is $-DS^2$ for integer spin values and $-D(S^2 - 1/2)$ for half integer spin values where S is the total spin number and D is the axial zero-field splitting parameter, associated to the magnetic anisotropy.

When, a compound of this kind, is subjected to a magnetic field one of the two wells becomes favoured and is preferentially populated (Fig.4, centre). When the external magnetic field is

removed at low temperatures, the magnetisation of the compound may remain (Fig.4, right) due to its energy barrier. The larger the U_{eff} value (which implies higher potential energy barrier), the slower relaxation magnetization therefore the system will return to thermal equilibrium in a longer period. Thus, a SMM requires a large *S* value in the ground state and/or a strong magnetic anisotropy (*D*) [10]. It is noteworthy that the behaviour of SMM stems from the intrinsic properties of the molecules. A large research effort has been done during the last decades into the design and synthesis of SMMs. A lot of complexes were synthesized with these magnetic properties based in others transition metals, for example: The case of Mn(III/IV) molecule that was the first molecule shown to be a SMM, was $[Mn_{12}O_{12}(O_2CMe)_{16}(H_2O)_4]\cdot 4H_2O\cdot 2HO_2CMe$ which exhibits slow magnetization relaxation thanks to a *S* =10 ground-sate split by axial zero-field splitting [8]. Because there is no possibility of increasing *D* an *S* at the same time, lanthanides have emerged as very good candidates to build SMMs thanks to their intrinsic single-ion anisotropy [11]. In this molecule, the relaxation was trough an over-barrier process, known as Orbach relaxation.

Another feature of the behaviour of SMM is the presence of a hysteresis cycle (Fig.3) in the response of the magnetization according to the extern magnetic field and that they present dependency of the imaginary susceptibility component with temperature and frequency when an altern magnetic field is applied to the system.

When the applied magnetic field is removed, the magnetization of the molecule can relax trough different relaxation mechanisms, known as Orbach, Raman, Direct and Tunnelling.

In the compounds presented in this work, two mechanisms are involved in the relaxation: Raman and direct process, (Fig.5) which, different to the abovementioned relaxation, do not involve an over-barrier relaxation process.

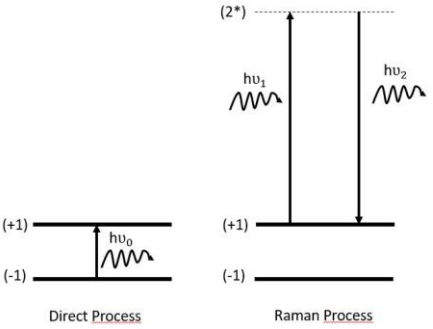

Fig 5. Plot of the Direct and Raman relaxation process.

The direct process is based on a spin system that relaxes by emitting one phonon with the same energy while the Raman process is based on the relaxation of magnetic moment involving a two-phonon process [12].

3.4. LUMINESCENCE

The studies of the luminescence of the complexes allow to investigate the electronic structures of these complexes and their absorption and emitting properties. In the simplest case, a compound has two electronic states with different energy and the electrons are in the lower state (ground state). When the compound is irradiated with a photon whose energy matches the energy difference between the two states, the compound promotes the electron to higher electronic state, called the excited state.

This state is not stable, and the compound spontaneously decays to the lowest, fundamental state, through a process called relaxation. The relaxation can be radiative (with emission of photons) or non-radiative (without the emission of photons, usually involving thermal processes). Furthermore, the radiative energy relaxation involves phosphorescence or fluorescence.

In the case of lanthanide complexes, because transitions in-between *f* states are Laporte forbidden, the ligands are used as chromophores. Chromophores are molecules, or part of a molecules, that absorb the visible or UV photons. Usually is a highly conjugated moiety, in our case the $BINAPO_2$ moiety.

In addition, for the photoluminescent system of compound, there are different selection rules which condition the intensity of the bands. The spin selection rule states that the promoted electron cannot change its spin during the transitions so, for example, the transitions between singlet-triple (S_0-T_1) states in organic ligands are forbidden. The Laporte rule states that the transitions within a symmetric orbital for example, the transition *f-f* are not permitted [13].

Fig.6 shows so-called Jablonski diagram, which depicts those process from organic chromophores.

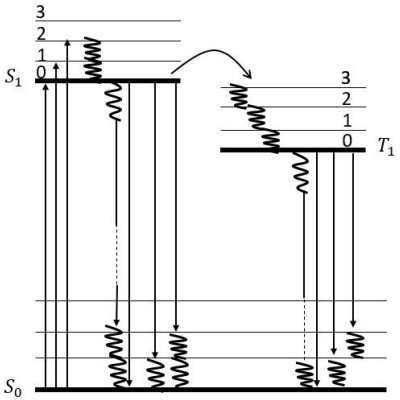

Fig.6. The Jablonski diagram for an organic chromophore. There are singlet and triplet exciting states (S_1 and T_1 respectively, and the ground singlet (S_0). Both the absorption and relaxation radiative processes are plotted with straight arrows, while the no radiative processes are plotted with undulated arrows.

After the absorption, the excited chromophore state presented an electron in the orbital HOMO (π) that has singlet multiplicity (S_0) and an electron in the orbital LUMO (π*) that can have singlet (S_1) or triplet (T_1). The state T_1 due to the spin inversion of electron, called intersystem crossing.

The difference between the two processes of radiative photoluminescent deactivation is that the fluorescence is given between the singlet S_1 and S_0 states of the chromophores. While the phosphorescence is given when the relaxation takes place from a triplet T_1 state to singlet S_0 state.

3.4.1. The sensitization effects

The direct absorptions of light between two spectroscopic *f* states of a lanthanide are very weak because *f-f* transitions are Laporte forbidden. As a result, 4*f* electrons are closer to the nucleus than the electrons in the 5*s* and 5*p* orbitals. To circumvent this situation, it is necessary to have strongly absorbent ligands coordinated to the Ln(III) ions, what we call the antenna effect. The antenna (organic ligand) helps in the absorption of light and transfers this energy to the excited state of the lanthanide. The, when this relaxes, the compound finally emits.

The energy transfer takes place from the excited triplet state of the ligand to the excited state of the metal. In theory, a ligand to metal charge transfer (LMCT) could also take place but is very unusual because of the high stability of the trivalent state of lanthanides. In addition, in ligands with more than one chromophore an intra-ligands CT (ILCT) can take place.

A requisite for obtaining an effective sensitization effect is the appropriate choice of the ligands. They must contain a good chromophore with a high absorption coefficient but also a good coordination group allowing a good interaction with the Ln(III) ion [14].

3.5. CHIRALITY

A chiral molecule is a molecule that cannot superpose with its specular image; the original molecule and the specular image have identical composition and connectivity. This is what we call *enantiomers*. Most of the properties of the enantiomers are identical but some of them such as the sense of the absorption of polarised light or the interactions with other chiral molecules are different. For example, life on Earth is essentially *chiral* in the sense that aminoacids, nucleosides and many other biomolecules are *homochiral*, i.e., Nature chose one enantiomer to form the biomolecules of all living organisms. Therefore, the topic of chirality is of utmost importance in the alimentary and pharmaceutical [15] industries and, more academically, in the search of the origin of life.

In this TFG the $BINAPO_2$ ligand is chiral and the coordination of the two enantiomers and of the racemic ligand were investigated. Regarding luminescence, the emitted light can be circularly polarised toward the left and to the right with different intensities. This process is called Circularly Polarized Luminescence (CPL).

4. OBJECTIVES

The objectives of this TFG project were:

I. Synthesis and characterization of the *rac*-$BINAPO_2$ (***rac*-1**) ligand.

II. Synthesis and characterization of Tb(III), Gd(III) and Eu(III) complexes with racemic and enantiopure $BINAPO_2$.

III. Study and rationalization of the magnetic properties of the lanthanide complexes.

IV. Study of the luminescent properties of the lanthanide complexes.

V. Study of the chiroptical properties of the lanthanide complexes.

5. EXPERIMENTAL SECTION

5.1. MATERIALS AND METHODS

All reagents and solvents were purchased from commercial sources and used without further purification.

The magnetic susceptibility and magnetization measurements for compounds [Tb(acac)$_3$((*R*)-BINAPO$_2$)] (**2a**), and [Gd(acac)$_3$((*R*)-BINAPO$_2$)] (**3a**) were performed with a Quantum Design MPMS-XL SQUID magnetometer at the Magnetic Measurements Unit of the Scientific and Technological Centres of the University of Barcelona (CCiTUB).

The single crystal X-Ray intensity data for compound **2a** was measured on a D8 Venture system equipped with a multilayer monochromator and a Mo microfocus (λ = 0.71073 Å) at the X-Ray Diffraction Unit of Scientific and Technological Centre of CCiTUB. The frames were integrated with the Bruker SAINT software package using a narrow-frame algorithm. The structure was solved and refined using the Bruker SHELXTL Software Package, using the space group P 41.

The infrared spectra were collected on Thermo Nicolett AVATAR 330 FT-IR spectrophotometer (4000 – 400 cm^{-1}) using potassium bromide pellets and the OMINC software program to process the IR spectra.

The ^{1}H and ^{31}P{^{1}H} NMR of compound **1** were collected in a 400 MHz Bruker Avance III spectrometer in $CDCl_3$. The spectra were processed with the MestReNova software.

The solid-state florescence spectra of compounds **2a**, [Tb(acac)$_3$(*rac*-BINAPO$_2$)] (**2c)** and [Eu(THMD)$_3$((*R*)-BINAPO$_2$)] (**4a)** were recorded on a Horiba Jobin Yvon SPEX Nanolog fluorescence spectrophotometer (Flurolog-3 v3.2, Horiba Jovin Yvon, Cedex, France) equipped with a three-slit, double grating excitation and emission monochromator with dispersions of 2.1 nm/mm (1200 grooves/mm) at room temperature. The steady-state luminescence was excited by unpolarized light from W xenon CW lamp and detected at an angle of 22.5º for solid-state measurements by a red-sensitive Hamamatsu R928 photomultiplier tube.

Circular dichroism measurements of compound **3a** and [Gd(acac)$_3$((*S*)-BINAPO$_2$)] (**3b)** were collected on a JASCO J-815 spectrometer, using a 1 cm path length quartz cuvette and a 400 – 200 nm wavelength range.

5.2. SYNTHESIS OF THE LIGANDS

5.2.1 *RAC*-BINAPO$_2$ (*RAC*-1)

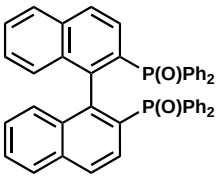

The first part of the synthesis must be carried out under exclusion of oxygen using a nitrogen-vacuum Schlenk line.

In a 250 mL Schlenk flask, *rac*-BINAP (5.00 g, 7.64 mmol) was dissolved in 50 mL of THF and cooled with an ice bath. A 30 % aqueous solution of hydrogen peroxide (30 mL) was added dropwise for 30 min and the mixture was left stirring for 4 h at room temperature. After this time, 50 mL of dichloromethane were added, and the aqueous phase was extracted with further dichloromethane (3 x 30 mL). The combined organic phases were dried with anhydrous sodium sulfate, filtered, and brought to dryness, giving the title product as a solid. Yield: 4.08 g (82 %).

White solid. **IR** ν (cm^{-1}): 1190 (P=O), 3050 (C=C-H). **^{1}H NMR**: δ 6.78-6.82 (m, 4H), 7.28-7.20 (m, 12H), 7.47-7.31 (m, 8H), 7.69 (ddd, *J* = 12.2,8.3,1.4 Hz, 4H), 7.81 (d, *J* = 8.2 Hz, 2H), 7.85 (dd, 2H). **^{31}P{^{1}H} NMR**: δ +28.3 (s).

5.3. SYNTHESIS OF THE LANTHANIDE COMPLEXES

The complexes of terbium(III), gadolinium(III) and europium(III) were synthesized following an analogous procedure by mixing the lanthanide salt and racemic or enantiopure BINAPO$_2$ (**1**). The syntheses were performed under standard, aerobic conditions.

5.3.1. Terbium(III) complexes

The synthetic procedure was the same for the two enantiomers and for the racemic compound. As a general procedure Tb(acac)$_3$·3H$_2$O (approximately 0.25 mmol) and BINAPO$_2$ (**1**) (approximately 0.25 mmol) were dissolved in 30 mL of acetone and refluxed (56 ºC) for 10 h under continued stirring. The solution evaporated under vacuum to reach half of its initial volume and 20 mL of hexane were added, causing the formation of a solid, which was filtered to give a yellow powder.

Yellow powder. **IR** ν (cm^{-1}): 1705 (m), 1434 (m), 1201 (s), 1116 (s), 752 (m), 641 (s), 576 (m).

Three syntheses were carried out, detailed in Table 1.

Table 1. Data for the syntheses of Tb(III) complexes.

Ligand 1	Ligand (g)	Tb(acac)$_3$·3H$_2$O (g)	Complex	Mass (g)	Yield (%)
(*R*)-BINAPO$_2$	0.165	0.127	JC17	0.265	95
(*S*)-BINAPO$_2$	0.143	0.123	JC29	0.218	90
(*rac*)-BINAPO$_2$	0.166	0.129	JC28	0.272	97

5.3.2. Gadolinium(III) complexes

The syntheses were analogous to those of terbium(III) complexes but using Gd(acac)$_3$·3H$_2$O (approximately 0.25 mmol) and racemic or enantiopure BINAPO$_2$ (**1**). The complexes were obtained as white powders.

White powder. **IR** ν (cm^{-1}): 1603 (s), 1511 (s), 1467 (m), 1435 (m), 1200(s), 1157 (m), 1116 (m), 725 (s), 700 (s), 517 (m).

Three syntheses were carried out and are detailed in Table 2.

Table 2. Data for the syntheses of Gd(III) complexes.

Ligand 1	Ligand (g)	Gd(acac)$_3$·3H$_2$O (g)	Complex	Mass (g)	Yield (%)
(*R*)-BINAPO$_2$	0.162	0.112	JC20	0.253	–[a]
(*S*)-BINAPO$_2$	0.162	0.112	JC27	0.267	–[a]
(*rac*)-BINAPO$_2$	0.164	0.116	JC21	0.272	–[a]

[a]The yield was not determined because the structure of the complex is not known.

5.3.3. Europium(III) complexes

The syntheses were analogous to those of terbium(III) complexes but using Eu(TMHD)$_3$·3H$_2$O (approximately 0.25 mmol) and racemic or enantiopure BINAPO$_2$ (**1**). The complexes were obtained as white powders.

White powder. **IR** ν (cm^{-1}): 1636 (m), 1435 (w), 1204 (s), 1117 (s), 753 (m), 723 (m), 698 (s), 516 (m).

Two syntheses were carried out, detailed in Table 3.

Table 3. Data for the syntheses of Eu(III) complexes.

Ligand 1	Ligand (g)	Eu(TMHD)$_3$·3H$_2$O (g)	Complex	Mass (g)	Yield (%)
(*R*)-BINAPO$_2$	0.162	0.175	JC18	0.253	–[a]
(*rac*)-BINAPO$_2$	0.161	0.174	JC19	0.272	–[a]

[a]The yield was not determined because the structure of the complex is not known.

6. RESULTS AND DISCUSSION

6.1. SYNTHESIS OF THE LIGANDS

Both *R* and *S* enantiomers of $BINAPO_2$ (**1**) were purchased in enantiopure form from commercial sources and used without further purification. However, *rac*-$BINAPO_2$ (***rac*-1**) is not commercially available and had to be prepared by oxidation of commercially available *rac*-BINAP with hydrogen peroxide in THF (Scheme 1) [14].

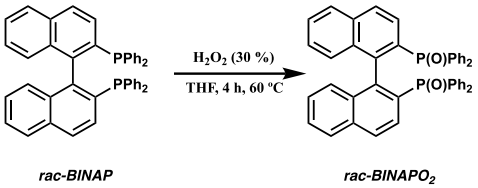

Scheme 1. The oxidation reaction of *rac*-BINAP to give ***rac*-1**.

The oxidation of *rac*-BINAP must be carried out under exclusion of oxygen using a nitrogen-vacuum Schlenk line. This may seem counterintuitive but although the oxygen of air could indeed perform the desired oxidation, its radicalary nature could also produce by-products, such as those bearing O insertions in P–C bonds; hence the oxidant should be solely hydrogen peroxide. After work-up, *rac*-$BINAPO_2$ (**1**) was obtained as a white powder.

The characterization of *rac*-$BINAPO_2$ was carried out by ^1H and $^{31}P\{^1H\}$ NMR spectroscopy and by infrared spectra (IR).

The ^1H NMR is shown in Fig.1 (Apx3). The analysis of each one of peaks that appear in the spectrum which it will be explain below.

First, it can be confirmed the naphthalene group and the benzene due to peaks which appear at the aromatic range (7-8 ppm). A doublet of doublets that corresponding to 2H at 7.85 ppm, a doublet at 7.81 (2H), a doublet of doublets of doublets at 7.69 ppm (4H), a multiplet, corresponding to 8H at 7.47-7.31 ppm, a multiplet, corresponding to 8H, at 7.28-7.20 ppm range and a multiplet that corresponding to 4H at 6.82-6.78 ppm range [16].

The $^{31}P\{^1H\}$ NMR is shown in Fig.2. (Apx3). The spectrum confirms the presence of a P=O group that appears as an intense singlet at δ +28.3 ppm, compared to shift of *rac*-BINAP (δ –15.6 ppm) [16]. It is well known that the oxidation of phosphines causes an increase of the chemical shift the $^{31}P\{^1H\}$ NMR spectra due to the reduced electron-richness of phosphorus.

Finally, the most important IR absorption band is the P=O stretching, which appears at 1190 cm^{-1} while another diagnostic band corresponds to C=C–H stretching and appears at 3050 cm^{-1} Fig.1. (Apx1).

6.2. SYNTHESIS OF THE LANTHANIDE COMPLEXES

The lanthanides salts used in this work have been terbium(III) acetylacetonate trihydrate, gadolinium(III) acetylacetonate trihydrate and 2,2,6,6-tetramethyl-3,5 heptanedionateeuropium(III) trihydrate. These salts were chosen based on previous group experience and literature precedents [17]. The 2,2,6,6-tetramethyl-3,5 heptanedionate (TMHD) ligands is a bulky version of the widely used acetylacetonate (acac) ligand and is shown in Fig.7.

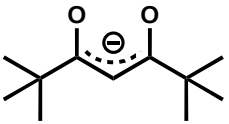

Fig.7. Structure of 2,2,6,6-tetramethyl-3,5 heptanedionate (TMHD) ligand.

The assignment of the most significant bands of compounds **2a**, **3a** and **4a** are shown in table 4.

Table 4. Selected absorption bands [cm^{-1}] from IR spectra of compounds **2a**, **3a** and **4a**.

Compound	ν(P=O)	ν(C=O)
2a	1201 (s)	1705 (m)
3a	1197 (s)	1603 (s)
4a	1204 (s)	1636 (m)

In addition, as is show in Fig.2, Fig.3 and Fig 4. (Apx1) in the range of 750-500 cm^{-1}, there is a significative absorption band at 516 cm^{-1} which corresponding to the band of the metal bond with the oxygen.

6.3. CRYSTAL STRUCTURES

To avoid repetitive descriptions, only the structure of [Tb(acac)$_3$((*R*)-BINAPO$_2$)] (**2a**) will be described because the complexes with *rac*-BINAPO$_2$ and (*S*)-BINAPO$_2$ are isostructural. The structures of Gd(III) compounds were in process of characterization while writing this TFG.

Complex **2a** (Fig.8) consists of a mononuclear system. The structure consists of a central Tb(III) cation coordinated to a single bidentate (*R*)-BINAPO$_2$ ligand and three acetylacetonate ligands, also acting as bidentate ligands.

Terbium cation is octacoordinated with a coordination sphere composed exclusively of oxygen atoms. Selected bond lengths and angles are listed in Table 2 (Apx.2). The vertexes of the coordination polyhedron are occupied by O atoms from the BINAPO$_2$ and acetylacetonate ligands. The O(1) and O(2) atoms from the BINAPO$_2$ are bound to the Tb(III) ion with Tb-O distances of 2.332 and 2.408 Å respectively, and the O(1)-Tb-O(2) angle is 69.04º. The O(3), O(4), O(5), O(6), O(7) and O(8) atoms from the acetyl acetonate ligands are bound with Tb(III) with distances in the range of 2.324 – 2.412 Å and the O-Tb-O angles from 68.52º to 145.75º. (Fig.2.)

The coordination geometry of the terbium atom can be defined either as a square antiprism (SAPR-8, Fig.9) or a bicapped trigonal prism (BTPR-8, Fig.10). The distortion of the coordination sphere of the Tb(III) ions has been calculated using the SHAPE V2 [23] program based on continuous shape measures (CShM). CShM allows us to determine the distances between the ideal coordination environment and our real structure, yielding a deviation from the ideal polyhedron of 1.052 and 1.056 respectively.

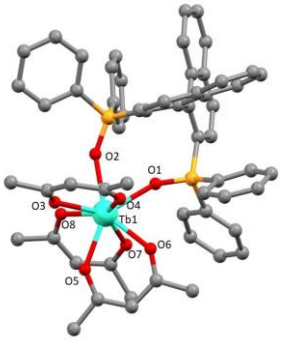

Fig.8. Partially labelled structure of (**2a**) Colour code: Grey = C, Red = O, Orange = P and Light blue/green =Tb. The hydrogen atoms omitted for clarity.

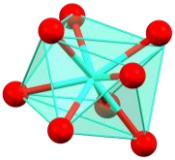

Fig.9. Coordination polyhedron of the terbium(III) atom in the mononuclear complex in compound **2a**. (SAPR-8).

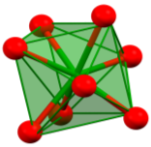

Fig.10. Coordination polyhedron of the terbium(III) atom in the mononuclear complex in compound **2a**. (BTPR-8).

6.4. MAGNETIC PROPERTIES

Susceptibility and magnetization measurements were performed only for the paramagnetic compounds **2a** and **3a** since europium(III) complexes **4a** and **4b** are diamagnetic.

6.4.1. STATIC MEASUREMENTS

The static magnetic susceptibility (χ_M) data for **2a** and **3a** was measured on polycrystalline and pressed samples in the 2-300 K temperature range and plotted as $\chi_M T$ vs. T (Fig.11). And fitted using PHI software [24].

At 300 K compound **2a** exhibit a $\chi_M T$ value of 12.17 $cm^3 \cdot mol^{-1} K$. This value is close to the expected value for a Tb(III) atom, which is 11.82 $cm^3 \cdot mol^{-1} K$ [18].

The curve of **2a** slightly decreases from 300 to 50 K, due the depopulation of the Stark sublevels, while at low temperatures the fall of the curve is due to antiferromagnetic intermolecular interactions or due to single ion anisotropy (*D*) effect by the Tb(III) ion or to the combination between both effects. The curve has been fitted using PHI software [24] and a Δ (assumable as *D*) value of –15.8 cm^{-1} has been found and a *z'J'* of 0.01 cm^{-1}.

A completely different behaviour is observed for the isotropic compound 3a. At 100 K compound **3a** exhibits a $\chi_M T$ value of 7.05 $cm^3 \cdot mol^{-1} K$. This value is close to the expected value for a Gd(III) atom, which is 7.88 $cm^3 \cdot mol^{-1} K$ for $S = 7/2$ [18]. On cooling the sample, $\chi_M T$ values remain constant up to 6 K because Gd(III) compounds follow the Curie's law. On further cooling, $\chi_M T$ values gradually decrease to 5.92 $cm^3 \cdot mol^{-1} K$ at 4 K probably due to antiferromagnetic intermolecular interactions.

The different behaviour of both compounds at low temperatures, evidences the differences in the anisotropy of the complexes. While **2a** shows the typical decay at low temperatures of the highly anisotropic compound induced by high *D* values, **3a** follows the Curie's law until χT curve

arrives almost to 2 K. This isotropic behaviour for **3a** is confirmed by the reduced magnetization values discussed below.

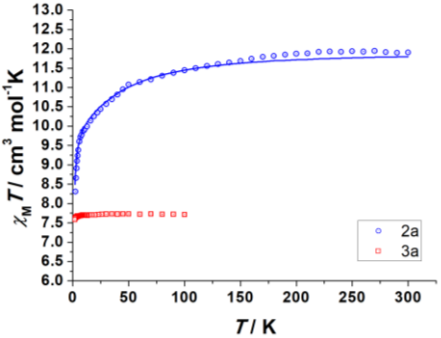

Fig.11. χ_MT vs temperature plots for complexes **2a** (blue circles) and **3a** (red squares). Solid lines show the best fit of the experimental data.

The field dependence of magnetization (*M*) of **2a** with the applied field was recorded at 2 K as shown in Fig.12. On increasing the external field, M values increase to a maximum value of 5.73 $N_{\mu B}$ at 7 T. The saturation value for a Tb(III) metal ions compound should be 6 $N_{\mu B}$.

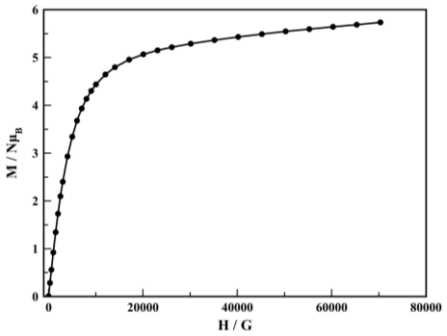

Fig.12. Magnetization vs. magnetic field at 2 K plot for compound **2a**.

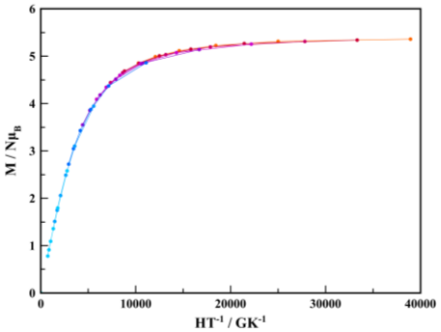

Fig.13. Reduced magnetization plot for compound **3a.** The solid lines are represented in different colours for showing the superimposable plots.

Reduced magnetization measurements between 1.8 and 5.8 K show superimposable plots evidencing a low or negligible axial anisotropy by the compound **3a**. (Fig.13) Among this, if the anisotropy is very slow, other techniques are needed to determine the exact value [19].

6.4.2. DYNAMIC MEASUREMENTS

Preliminary AC's measurements at zero field indicated a fast relaxation of the magnetization for all compounds, meaning no SIM behaviour. However, **3a** shows susceptibility dependence of the temperature at different applied fields.

For compound **3a**, the AC studies were performed in a dc external magnetic field of 0.3 T in a temperature range of 1.8 to 11.92 K and frequencies in the range 1.00-1488.09 Hz.

As is shown in Fig.14 and Fig.15 the compound **3a** shows temperature and frequency-dependent behaviour both in-phase and out-of-phase (χ_M' and χ_M'' respectively) revealing slow magnetic relaxation behaviour which is considered a fingerprint of field-induced Single Ion Magnets (SIMs) [19], [20].

In the plot of χ_M'' (out-of-phase susceptibility) versus temperature (Fig. 14) it can be observed the typical maximum that demonstrated that the compound **3a** has slow relaxation (and it can be differentiated the range at low frequencies and at high frequencies) while in Fig. 15 the dependence of χ_M'' is shown in front of the frequency.

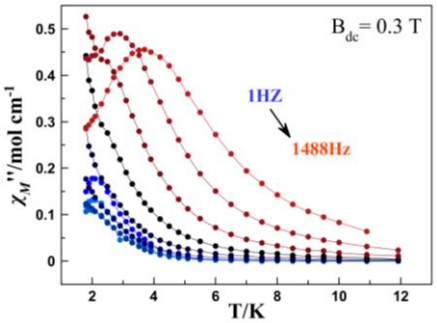

Fig.14. The temperature dependence of χ_M'' for compound **3a** at optimal applied external magnetic fields of 0.3 T. Low frequency region is represented in blue while high frequency region is represented in red.

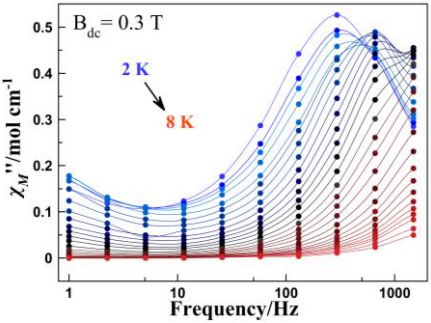

Fig.15. The frequency dependence of χ_M'' for compound **3a** at optimal applied external magnetic fields of 0.3 T. Low temperatures region is represented in blue while high temperature region is represented in red.

To elucidate the relaxation process of **3a**, the Cole-Cole or Argand plots were represented.

These plots represented the imaginary versus the real component of the susceptibility. (Fig.16). These plots allow us to elucidate the relaxation mechanisms of the system by using the generalized Debye model.

$$\chi_{ac}(\omega) = \chi_{S,tot} + \frac{X_{T1}-X_{S1}}{1+(i\omega\tau_1)^{1-\alpha_1}} + \frac{X_{T2}-X_{S2}}{1+(i\omega\tau_2)^{1-\alpha_2}} \quad \text{(Eq.9.)}$$

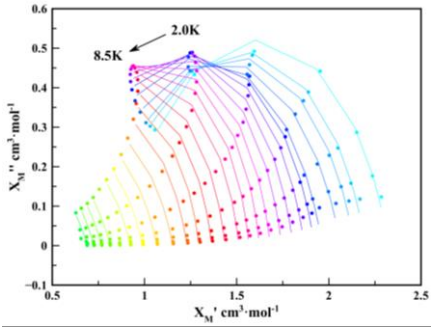

Fig.16. Argand plot of the magnetic susceptibility for compound **3a**.

The data extracted from the fitting of the Cole-Cole plot using equation 10 (CCfit software [24]), is represented in the form of ln(τ) vs. 1/T (Fig.17). Two relaxations can be observed: the data was simulated following the combination of Raman plus Direct relaxations, respectively, first and second term of Eq.10.

$$\tau^{-1} = C \cdot T^n + A \cdot T \qquad \text{(Eq.10.)}$$

Best fitting parameters are C = 19.9 $s^{-1} \cdot K^n$, n = 3.9 and A = 1267.4$s^{-1} \cdot K1$, with C and A as fitting constants and n as the Raman coefficient.

It is noteworthy that the Gd(III) complex **3a** exhibit strong out-of-phase signals despite its spherical electronic distribution and apparently isotropic character. In principle, this feature goes against one of the paradigms of the SMMs, which supposed to need strong anisotropy. However, many some examples can be found in the literature reporting this behaviour in isotropic compounds [21].

This field-induced slow relaxation in the Gd compound, is probably due to the existence of ta small anisotropy, not detectable with magnetometry measurements.

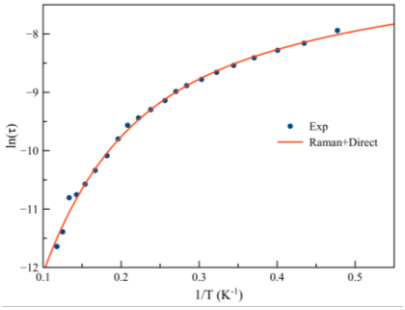

Figure.17. Temperature dependence of the relaxation time as function of the temperature plotted as ln(τ) vs. inverse of T. Solid lines show the best fit of the experimental data (Raman plus Direct fitting) and dotted lines show the experimental dates which obtained in the magnetic measurements.

6.5. LUMINESCENT PROPERTIES

The emissive properties of compounds **1**, **2a** and **4a** have been studied in polycrystalline samples. The compounds of Gd(III) have the 4*f* half-filled shell with 7 electrons. The energy difference between the first excited electronic state ($^6P_{7/2}$) and the fundamental state ($^8S_{7/2}$) of the Gd(III) ion is rather high. For this reason, the sensitization of the gadolinium emission does not happen with the conventional organic ligands since the excited state of those is lower in energy than the emitting level of cation Gd(III).[10]

6.5.1. SPECTRA OF LIGAND 1

The excitation and emission spectra for **1** are represented in Fig.18 (left) and Fig.18 (right) respectively. When the exciting the ligand at the excitation wavelength (λ_{ex}) of 346 nm are intense and broad emission band appears at 369 nm. The fluorescent band is assigned to the $\pi^* \rightarrow \pi$ transitions of the aromatic part.

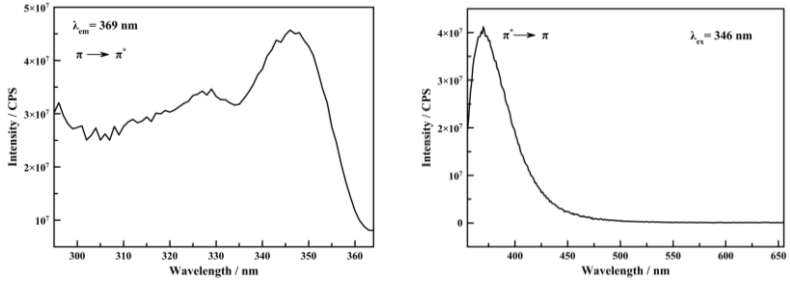

Fig.18. Excitation (left) and emission (right) spectra of compound **1**

6.5.2. EXCITATION SPECTRA OF TERBIUM(III) AND EUROPIUM(III) COMPLEXES

The excitation spectrum measured at λ_{em} of 544 nm (Fig. 19 (left)) corresponding to compound **2a** and the excitation spectrum measured at λ_{em} of 611 nm (Fig.19 (right)) corresponding to compound **4a**.

The broad bands of both spectra correspond to the π-π* and n-π* transitions from the naphthalene groups of the ligand **1**. These excitation spectra suggest an efficient sensitization effect since the intensity of the excitation bad is rather high.

Besides, those type of broad-bands are characteristic of the organic-ligands due to the vibration coupling called Frank-Condon principle. This principle is related with the movement of the bonds when the compound is excited in relation to initial compound [10].

Furthermore, independently of the photoluminescent system of the compound exist different selection rules that run into the intensity bands which are related as much the emission process as absorption process.

It should be pointed out that the π-π* organic transition of type S_0-S_1 are both spin and Laporte allowed transitions and for this reason the bands are the very intense.

Recently, it has been publicised an article which a series of polymeric lanthanide compounds are described. The ligand is formed by different phosphines that have been presented in this work. For these compounds were done the luminescent study as much the ligand as the lanthanide compounds in solid state. It was concluded that the sensitization effect was not effective since the excitation spectra appeared bands that corresponding to the excitation of the metal which come from the *f-f* lanthanide transitions. And these are more intense that the band of the own ligand [10].

In conclusion, it can be deduced by the bibliography that the compound **2a** and **4a** have an efficient sensitization effect.

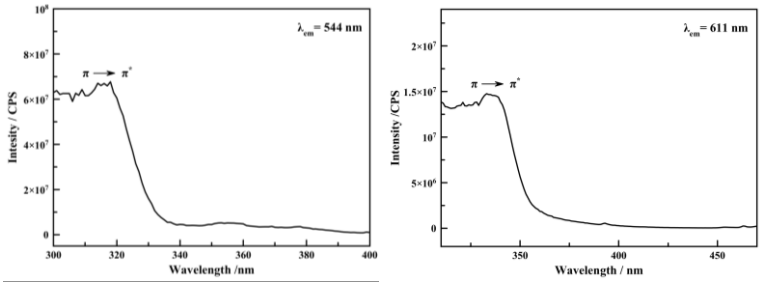

Fig.19. Excitation spectra of compound **2a** (left) and the excitation spectra of compound **4a** (right).

6.5.3. EMISSION SPECTRA OF TERBIUM(III) AND EUROPIUM(III) COMPLEXES

The emission spectra of the terbium compound (**2a**) measured at λ_{ex} of 316 nm (ligand excitation) induced emission and the expected band from *f-f* transitions are discerned at 491, 546, 583 and 618 nm, consistent with the radiative transitions from the $^5D_4$ emitting energy level to the $^7F_{6-3}$ ground state, respectively. Among this, very weak bands corresponding to $^5D_4 \rightarrow {}^7F_{2-1}$ transitions are perceived in the 650-700 nm range. All these bands are shown in Fig.20 [22].

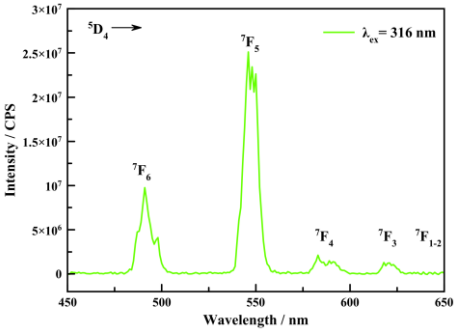

Fig.20. The emission spectra of compound **2a**.

On the other hand, the emission spectra of the europium compound (**4a**) measured at λ_{ex} of 335 nm (ligand excitation) is given in Fig.20. The bands corresponding to the emission from the $^5D_0$ emitting energy level at 580, 597 and 612 nm are in good agreement with the $^5D_0 \rightarrow {}^7F_{(0-3)}$ transitions.

The magnetic dipole $^5D_0 \rightarrow {}^7F_1$ transition, whose intensity is independent from its environment, is split due to the crystal field and this splitting is manifested as a shoulder. Then, the most intense band corresponds to the electric dipole $^5D_0$ $^7F_2$ transition [20].

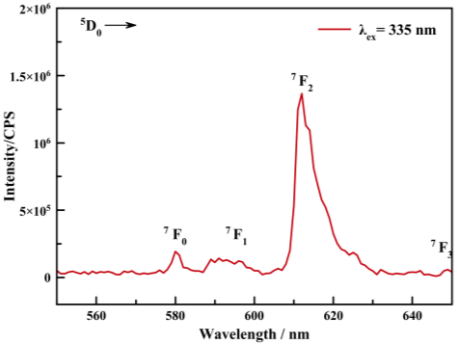

Fig.20. The emission spectra of compound **4a**.

In conclusion, from the emission spectra it can be deduced that both compounds **2a** and **4a** have emissive bands and an effective sensitization effect. Due to that, the only signals that appeared in the both spectra are the *f-f* transitions from terbium(III) and europium(III).

6.6. CHIRALITY PROPERTIES

Chirality transfer is a common feature when using enantiopure chiral ligands in coordination compounds, as is the case of the complexes which have been synthesized in this TFG project. The chirality studies have been realised in the Gd(III) compounds, specifically compounds **3a** and **3b**. The chiroptical properties must be mainly related to the ligands due to the π-π* transitions of the aromatic rings from the enantiopure $BINAPO_2$ ligand.

The electronic circular dichroism spectra in methanol solution were recorded for the representative enantiomeric pairs of **3a** (with the ligand **(*R*)-1**) and **3b** (with the ligand **(*S*)-1**) are given in Fig.21. Their mirror image confirms the enantiomeric nature of the reported complexes.

The spectrum exhibits a positive Cotton effect at λ_{max} 239.5 nm and a negative band at 241 nm for **3a** and the same band with opposite sign for **3b.** In addition, at 207.05, 225.5, 270, 301.5 and 333 nm appear bands with low intensity for **3a** and the same bands with opposite sign for **3b** [21].

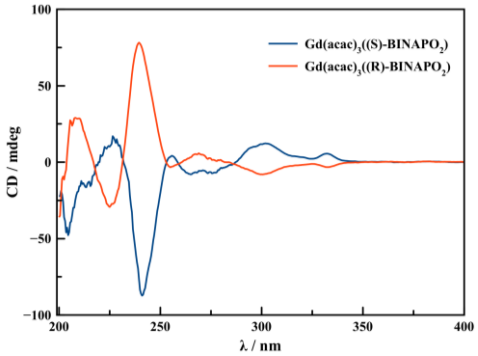

Fig.21. Solution ECD spectra for the Gd^{III} pair of complexes **3a** (red line) and **3b** (blue line).

7. CONCLUSIONS

Ligand *rac*-**1** was easily obtained by oxidation of *rac*-BINAP with hydrogen peroxide in good yield. The complexation of enantiopure and racemic **1** to terbium(III), gadolinium(III) and europium(III) salts have given eight complexes, that have been characterised by several techniques.

The complex **2a** is a neutral mononuclear species with the formula [Tb(acac)$_3$((*R*)-**1**)], with **1** acting as a bidentate ligand by the phosphoryl groups. The complex is octacoordinated to 8 oxygen atoms and the coordination geometry can be described either as a square antiprism (SAPR-8) or a bicapped trigonal prim (BTPR-8).

The magnetic measurements indicate that **2a** presents an antiferromagnetic intermolecular interaction and a high intrinsic single ion anisotropy due to terbium(III) and it does not present SIMs behaviour. The **3a** compound with Gd(III) is isotropic and it presents SIMs behaviour despite that theoretical calculations do not predict this character. This can be rationalised by the low *D* value of the complex.

The luminescent measurements show that the *rac*-**1** is a chromophore group as expected and that complexes **2a** and **4a** presented an effective sensitization effect.

Finally, the chiroptical properties have been studied by Gd(III) complexes **3a** and **3b**, containing the *R* and *S* enantiomers of **1** respectively. It has been found that the circular dichroism spectrum is given by the π-π^* transitions of the aromatic rings of **1**. As expected, the two spectra are mirror images, which confirms the analogous structure of **3a** and **3b**.

8. REFERENCES AND NOTES

1. L. Ouahab,"Ed. Multifunctional molecular Materials", CRC Press Taylor & Francis Group, *Boca Raton*, **2013**.
2. S. V. Elisseva, and J.C.G. Bünzli, *Chem. Soc. Rev*., **2010**, 39, 189-227.
3. D. A. Atwood, Ed., "The Rare Earth Elements," *John Wiley & Sons*, Ltd, **2012** pp. 43-81.
4. A. Miyashita, A. Yasuda, H. Takaya, K. Toriumi, T. Ito, T.Souchi, and R. J. Noyori, *J. Am. Chem. Soc*. **1980**, 102, 7932-7934.
5. M. Berthod, G. Mignani, G. Woodward, and M. Lemaire, *Chem. Rev*., **2005**, 105, 1801-1836.
6. A. W. G. Platt, *Coord. Chem. Rev*., **2017**, 340, 62-78.
7. J. Ribas, "Coordination,Chemistry", Whiley-VCH, **2008**.
8. J. Yoo, E. K Brechin, A. Yamaguchi, M. Nakano, J. C. Huffman, A. L. Maniero, L. C. Brunel, K. Awaga, H. Ishimoto, G. Christou, and D. N. Hendrickson, *Inorg. Chem.* **2000**, 39, 3615-3623.
9. D. Gatteschi, R. Sessoli, and J. Villa, "Molecular nanomagnents", *OUP Oxford* **2006** pp.49-81.
10. D. Gatteschi, R. Sessoli, and J. Villa, "Molecular nanomagnents", *OUP Oxford* **2006** pp.108-156.
11. J. Tang, and P. Zhang, "Lanthanide Single Molecule Magnets", *Springer Berlin Heidelberg*, Berlin, Heidelberg, **2015**.
12. D. Aravena and E. Ruiz, *Dalton Trans.*, **2020**, 49, 9916-9928.
13. D. A. Atwood, Ed., "The Rare Earth Elements," John Wiley & Sons, Ltd, **2012** pp. 111-133
14. G. Muller, *Dalton. Trans.*, **2009**, 9692-9707.
15. Q. Sun, X. Meng, X. Liu, X. Zhang, Y. Yang, Q. Yang, and F.S. Xiao, *Chem. Commun.*, **2012**, 48, 10505-10507.
16. C. Laye, C. Lusseau, J. Robert, and F. Y. Landais, *Adv. Synth. Catal.*, **2021**, 363, 3035-3043.
17. M. Abdus Subhan, Y. Hasegawa, T. Suzuki, S. Kaizaki, and Y. Shozo*, Inorg. Chim. Acta*, **2009**, 362, 136-142.
18. J. Mayans, and A. Escuer, *Chem. Commum*., **2021**, 57, 721-724.
19. D. P. Li, T. W. Wang C. H. Li, D. S. Liu, Y. Z. You, and X. Z. Li, *Chem. Commun*., **2010**, 46, 2929-2931.
20. M. Pietraszkiewicz, S. Mal, O. Pietraszkiewicz, K. Górski, and N. Chelwani*, Zeit. Naturforsch. B*, **2014**, 69, 239-247
21. E. Pilichos, M. Font-Bardia, A. Escuer, and J. Mayans*, Dalton Trans*., **2021**, 50, 1746-1753.
22. A. P. S. Samuel, J. Xu, and K. N. Raymond, *Inorg. Chem*., **2009**, 48, 687-689.
23. SHAPE v.2.0. M. Llunell, D. Casanova, J. Cirera, P. Alemany, and S. Alvarez, Barcelona **2010**. The program can be obtained by request to the authors.
24. N. F. Chilton, R. P. Anderson, L. D. Turner, A. Soncini and K. S. Murray, *J. Comput. Chem*., **2013**, 34, 1164-1175.

9. ACRONYMS

acac: acetylacetonate

BINAP: 2,2'-bis(diphenylphosphino)-1,1'-binaphthalene

$BINAPO_2$: 2,2'-bis(diphenylphosphino)-1,1'-binaphthalene dioxide

CPL: Circularly Polarized Light

ECD: Electronic Circular Dichroism

IR: Infrared Spectroscopy

NMR: Nuclear Magnetic Resonance spectroscopy

SMM: Single Molecular Magnet

SIM: Single Ion Magnet

TMHD: 2,2,6,6-tetramethyl-3,5-heptanedionate

APPENDICES

APPENDIX 1: IR SPECTRA

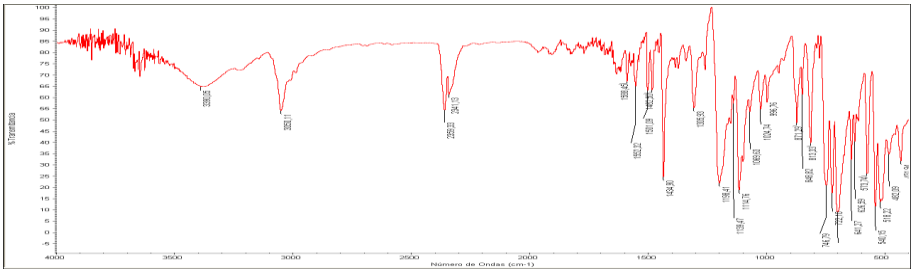

Fig.1. (Apx1.) IR spectrum of *rac*-$BINAPO_2$. **(1)**

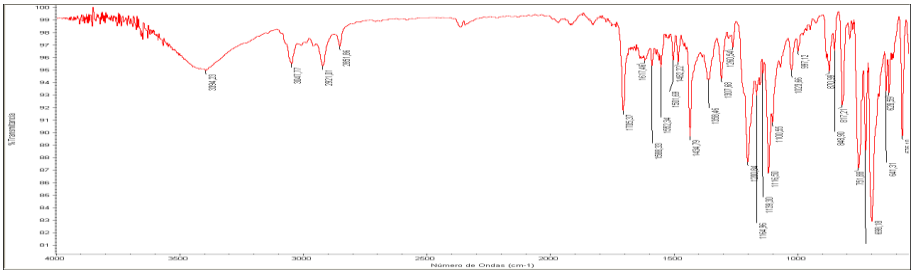

Fig.2. (Apx1). IR spectrum of $[Tb(acac)_3((R)\text{-}BINAPO_2)]$ (**2a**)

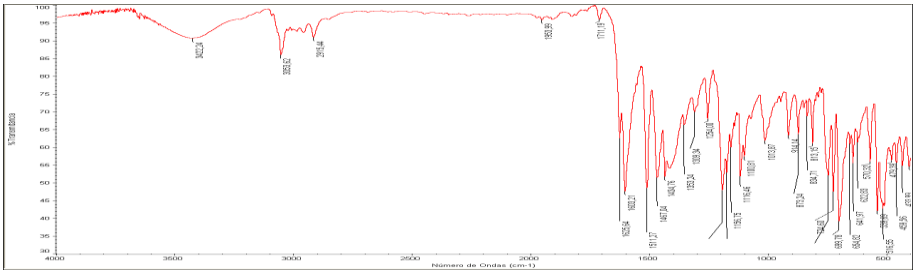

Fig.3. (Apx2). IR spectrum of $[Gd(acac)_3((R)\text{-}BINAPO_2)]$ (**3a**)

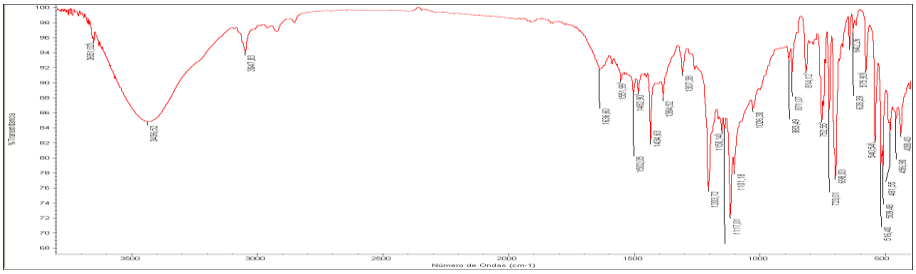

Fig.4.(Apx1).IR spectrum of $[Eu(THMD)_3((R)\text{-}BINAPO_2)]$ (**4a)**

APPENDIX 2: CRYSTAL DATA AND SELECTED BOND LENGTHS AND ANGLES FOR COMPOUND 2A.

Crystal Data	Compound
Formula	$C_{59}H_{53}O_8P_2Tb$
FW [g/mol]	1110.87
Crystal System	Tetragonal
Space group	P41
a [Å]	a = 12.9939 (2)
b [Å]	b = 12.9939 (2)
c [Å]	c = 29.5493 (6)
α [deg]	90
β [deg]	90
γ [deg]	90
V [Å³]	4989.15 (18)
Z	4
ρ_{calc} [g/cm³]	1.479
μ(Moka) [mm⁻¹]	1.539
F(000)	2264
Crystal Size [mm]	0.125 x 0.094 x 0.064

Table 1 (Apx.1). Crystal Data and Details of the Structure Determination of compound **2a.**

Atoms	Distances [Å]	Atoms	Distances [Å]
Tb1-O6	2.324 (2)	**Tb1-O5**	2.369 (2)
Tb1-O7	2.330 (2)	**Tb1-O3**	2.388 (7)
Tb1-O1	2.332 (2)	**Tb1-O2**	2.408 (2)
Tb1-O8	2.340 (2)	**Tb1-O4**	2.412 (3)

Table 2 (Apx.2) Selected bond lengths for compound **2a**.

APPENDIX 3: ^{1}H AND $^{31}P\{^{1}H\}$ RMN

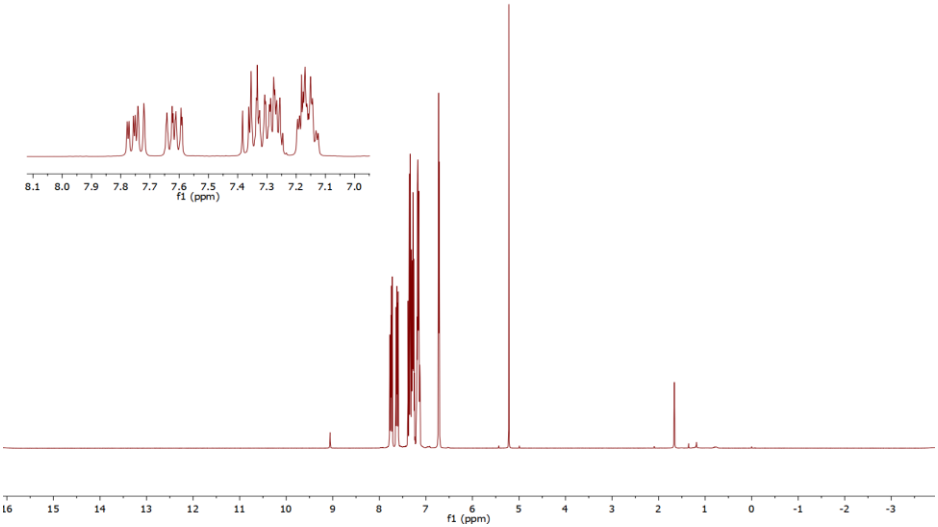

Fig.1. (Apx.3) ^{1}H RMN of *rac*-BINAPO$_2$. (1)

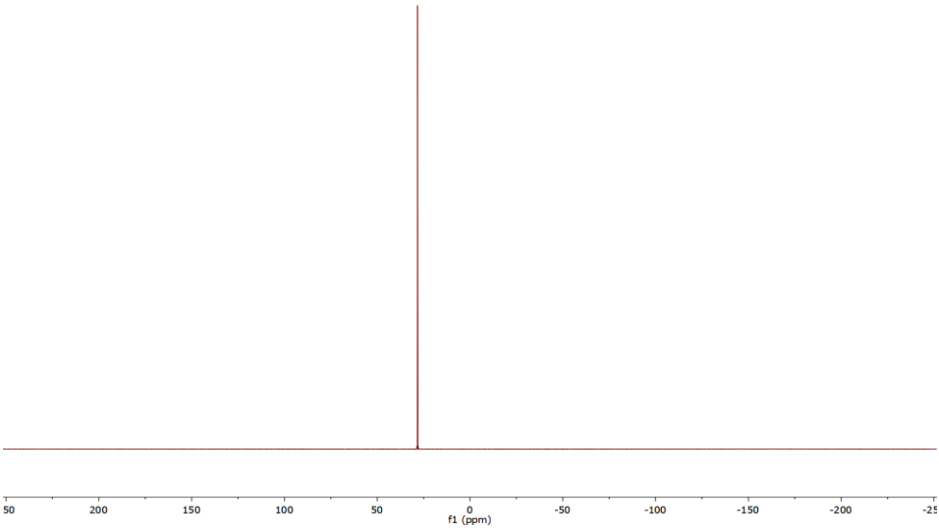

Fig.2. (Apx.3) 31P{1H} RMN of rac-BINAPO$_2$. (1)